A Data-driven Method to Control Buildings Sub-zones to Spatio-temporal Profiles

Aayushman Sharma, Raman Goyal, Saman Mostafavi, Shamus Li, Alejandro E Brito, Eric Bier
Palo Alto Research Center (PARC), Palo Alto, California, USA

Abstract

In this paper, we present a data-driven approach for optimally controlling sub-zonal, spatiotemporal temperature profiles in spacious rooms. Our methodology begins with the calibration of a 2D diffusion Partial Differential Equation (PDE) model for heat transfer, utilizing Bluetooth Low Energy (BLE) sensor data (temperature and humidity) gathered from an experimental testbed. This calibrated model serves as the basis for an iterative Linear Quadratic Regulator (iLQR) algorithm, which generates optimal control policies for each receding horizon in a model predictive control framework. We demonstrate the effectiveness of our nonlinear control approach in maintaining desired spatiotemporal temperature profiles while mitigating the effects of external disturbances and noise. Our simulation results showcase the feasibility of optimally controlling heating systems to achieve desired temperature distributions across various regions of a room. This data-driven method contributes to the development of more efficient and responsive building control systems that cater to occupant preferences and comfort.

Highlights

- Development of a data-driven approach for optimal control of sub-zonal, spatiotemporal temperature profiles in spacious rooms.
- Implementation of iLQR algorithm within a model predictive control framework for nonlinear control performance.
- Effective mitigation of external disturbances and noise through feedback control strategies.
- Simulation results demonstrate feasibility and potential for more efficient, responsive building control systems tailored to occupant preferences and comfort.

Introduction

Buildings consume a significant portion of global energy resources, with heating, ventilation, and air conditioning (HVAC) systems contributing a considerable share of this consumption. As concerns over energy efficiency, sustainability, and occupant comfort increase, there is a growing need for innovative approaches to building control systems that optimize energy usage while maintaining desired indoor environmental conditions. Many buildings, ranging from commercial spaces with large auditoriums to data centers, exhibit non-uniform heat ventilation and heat generation, providing an excellent opportunity for customized control at sub-zonal levels.

In recent years, the concept of sub-zonal control has emerged as a promising solution for improving building energy efficiency and occupant satisfaction. Sub-zonal control focuses on regulating temperature profiles in individual regions or zones within a room, enabling more precise control and customization according to occupant preferences. Several state-of-the-art approaches for customized sub-zonal control focus on simulation-assisted strategies (Tian et al. (2018); Zhai et al. (2002); Wetter et al. (2015)), while others have shifted their focus towards PDE models to address the limitations of ODE-based predictive control in providing detailed control of airflow and temperature in HVAC systems.

PDE-based heat control in buildings

Despite the complexity of airflow dynamics, laminar behavior can be observed in larger areas (Sinha et al., 2000), enabling the use of simpler non-turbulent Computer Fluid Dynamics (CFD) models. He and Gonzalez (2016) developed a gradient-based estimation algorithm for real-time temperature distribution and geometric configuration estimation in buildings. Thong (2023) introduced a smart adaptive vent (SAV) system verified on CFD simulations to reduce energy consumption through targeted air conditioning. Other researchers have explored coupled simulations of HVAC control systems and envelope CFD models to achieve simulation-assisted performance analysis (Zuo et al., 2016; Qiao et al., 2019). Importantly, these models can be coupled with gradient-based optimization algorithms under suitable conditions, due to the existence and smoothness of their solutions (Sinha et al., 2000; Van Schijndel, 2011), making them a suitable option for model-based predictive controls.

There are two significant limitations in existing studies: (a) although these models offer certain advantages, integrating them with gradient-based optimization algorithms is challenging due to the need for explicit formulation of all approximating equations and their gradients, leading to less studied control of such systems with the notable exception of Runxin and Humberto (2016). (b) The development of a data-driven real-time control system that leverages sensor data from multiple locations and accommodates the varying preferences of occupants in different sub-regions has yet to be clearly established.

https://doi.org/10.26868/25222708.2023.1421

Scientific Innovation and Relevance

The field of control of infinite-dimensional PDEs has a rich history (Casas et al. (2022); Casas and Kunisch (2022); Volkwein (2001); Banholzer et al. (2020); Smyshlyaev and Krstic (2010); Alla and Falcone (2013); Alla and Volkwein (2015)). This foundational work was further built upon for application to nonlinear PDE control (Stoll and Breiten (2015), Baumann et al. (2018), Leibfritz and Volkwein (2007), Griesse and Volkwein (2005), Krstic and Smyshlyaev (2008)). Despite that, the issues that plague the tractability of solving these problems still persist.

Optimal control of a nonlinear dynamical system, particularly those with continuous state and action spaces, poses a significant challenge due to the "curse of dimensionality" inherent in dynamic programming (DP) problems, especially when based on PDEs (Kumar and Varaiya, 2015). Controlling heat-diffusion PDEs is computationally intractable using current model-free approaches, specifically, Reinforcement Learning (RL). It is often data-intensive, requires extensive training time, and suffers from high variance and reproducibility issues that impact its performance (Henderson et al. (2018)). Additionally, for model-based methods, the granular data necessary to identify a control-oriented model is not readily available within the building management system data streams.

This work paves the way for a systematic feedback control synthesis approach specifically tailored for data-driven control of heat-diffusion PDEs. We introduce a novel data-driven modeling and control method that hinges on our in-house sensor commissioning system[1], enabling rapid and reliable data collection. This, in turn, allows us to identify data-driven PDE models and restructure them as model predictive control (MPC) problems for monitoring temperature profiles. Our approach's robustness and scalability, as well as its ability to adapt to changes in sensor locations and control profiles, make it suitable for larger applications such as auditorium spaces and data centers.

Heat Diffusion Model Calibration with Experimental Data

In this section, we present the non-linear dynamics model for two-dimensional (2D) heat flow in a room and discuss the calibration process of the partial differential equation (PDE) models using real sensor data obtained from an experimental test-bed.

2D Heat Transfer PDE

The general form of the heat-transfer equation is given by:

$$\frac{\partial \theta(x,t)}{\partial t} = \nabla.(\alpha(\theta)\nabla\theta(x,t)) + u(x,t), \tag{1}$$

[1]The authors have submitted a paper explaining their sensor commissioning and data collection methods in detail. To comply with the double-blind review process, we have removed this information from the submission currently under review and plan to add it back upon acceptance.

where α denotes the thermal diffusivity, $\theta = \theta(x,t)$ represents the spatio-temporal temperature profile, and $u(x,t)$ is the external actuation (e.g., heaters/coolers) applied across the grid. In control terminology, θ serves as the state of the system and is an infinite-dimensional, spatio-temporally varying function. For a homogeneous system, the thermal diffusivity is generally independent of temperature variation. Consequently, Eq. 1 simplifies to the following parabolic PDE:

$$\theta_t = \alpha\nabla^2\theta(x,t) + u(x,t). \tag{2}$$

Discretized model for PDE control

We discretize the phase-field into a 2D grid of dimension $N \times N$. Let $\theta_t^{i,j}$ denote the phase field of the cell defined by grid location (i,j) for all $i,j = \{1,...,N\}$, at time t. Employing a central-difference scheme based on Eq. (1), we obtain the high-dimensional 2D phase-field model. Rearranging the terms results in the following expression for the time-variation of the local phase-field:

$$\theta_{t+1}^{i,j} = \theta_t^{i,j} + \alpha\Delta t\left(\frac{\theta_t^{i+1,j} + \theta_t^{i-1,j} + \theta_t^{i,j+1} + \theta_t^{i,j-1} - 4\theta_t^{i,j}}{\Delta x^2}\right) \tag{3}$$

with the boundary conditions $\theta_t^{i,N} = T_{right-wall}(t)$, $\theta_t^{i,0} = T_{left-wall}(t)$, $\theta_t^{0,j} = T_{upper-wall}(t)$ and $\theta_t^{N,j} = T_{lower-wall}(t)$. For any given time t, the temperature profile vector θ_t and the control input vector u_t can be defined as a stack of all states $\theta_t^{i,j}$ and control inputs $u_t^{i,j} = T_t^{i,j^T}$, respectively. Using Eq. (3), we can simulate the phase-field at the subsequent time step. Furthermore, the dynamics are affine in control.

The system can, thus, be described in the discretized state-space form as:

$$\Theta_{t+1} = f(\Theta_t) + g(\Theta_t)U_t, \tag{4}$$

where $\Theta_t = \{\theta_t^{i,j}\}$ is the phase variable on the spatially discretized FD grid at time t, and $U_t = \{u_t^{i,j}\}$ represents the control variables on the same grid at time t.

Calibration of the discretized PDE model

We first collect data from sparse temperature sensors to fit a spatio-temporal temperature profile with piecewise cubic interpolation. The PDE model was then calibrated by first discretizing the heat diffusion model both in space and time on a regular grid and then using the spatio-temporal temperature data to find the coefficient of thermal diffusivity α using least square estimation.

To interpolate the data from sparse sensors onto a regular grid (Fig. (1)), we use a triangle-based C^1 interpolation method (Renka et al., 1984) involving the following steps:

1. Delaunay triangulation: Construct a triangulation of the input data points in the (x,y)-plane, with the most common choice being the Delaunay triangulation, which ensures that no input point is inside the circumcircle of any triangle in the triangulation.

https://doi.org/10.26868/25222708.2023.1421

2. Define a local coordinate system for each triangle: For each triangle in the triangulation, introduce a local coordinate system (u,v), where u and v are barycentric coordinates, satisfying:

$$u+v \leq 1, u \geq 0, v \geq 0. \tag{5}$$

3. Construct a polynomial function on each triangle: For each triangle, find a bivariate polynomial function $S(u,v)$ that interpolates the data points in the local coordinate system. The polynomial function must satisfy the continuity conditions:

$$S(u,v) = \sum_{i=0}^{n}\sum_{j=0}^{n} a_{ij} u^i v^j, \tag{6}$$

where a_{ij} are the coefficients of the polynomial, and n is the degree of the polynomial. The coefficients must be chosen so that the function $S(u,v)$ and its first-order derivatives match the given data points and their gradients.

4. Combine the local polynomials to form a global interpolating surface: After constructing a polynomial for each triangle, assemble them to create a continuous and smooth interpolating surface in the entire domain.

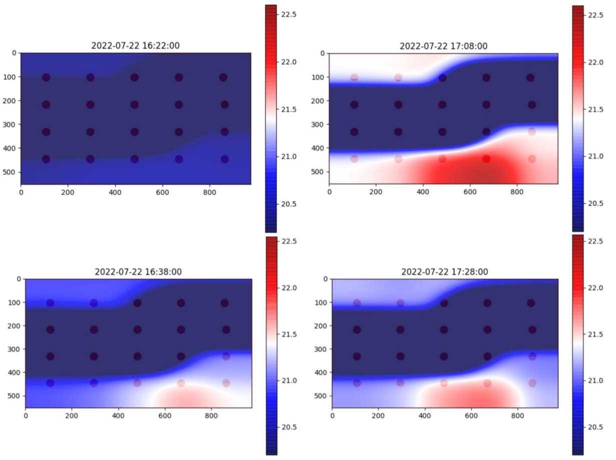

Figure 1: Heat profile visualization obtained from temper ature data collected in a tabletop experiment using BLE s ensors, with the described triangle-based C^1 interpolatio n method applied.

Control Problem Formulation

This section focuses on the optimal control of high Degree of Freedom (DoF) heat-diffusion Partial Differential Equations (PDEs). The heat-diffusion model is complex, nonlinear, and high DoF, which makes it difficult to obtain analytical solutions. Consequently, data-based approaches are a natural choice for controlling these systems. We employ a highly efficient method (compared to RL) to solve the problem in a completely data-based manner. The approach involves two steps: (i) optimizing the nominal open-loop trajectory of the system using a 'black-box simulation' model, and (ii) identifying the linear system governing perturbations from the nominal trajectory using random input-output perturbation data, followed by designing an LQR controller for this linearized system. We present a general nonlinear formulation of the optimal control problem for a discrete-time nonlinear dynamical system: Consider the discrete-time nonlinear dynamical system:

$$\theta_{t+1} = f(\theta_t, u_t), \tag{7}$$

where $x_t \in \mathbb{R}^{n_\theta}$ and $u_t \in \mathbb{R}^{n_u}$ correspond to the state and control vectors at time t. The optimal control problem is to find the optimal control policy $\pi^0 = \{\pi_0^0, \pi_1^0 \ldots \pi_{T-1}^0\}$, that minimizes the cumulative cost:

$$\min_{\pi} J^{\pi}(\theta) = \sum_{t=0}^{T-1} c_t(\theta_t, u_t) + c_T(\theta_T), \tag{8}$$

$$\text{Subject to: } \theta_{t+1} = f(\theta_t, u_t), \tag{9}$$

given some $\theta_0 = \theta$, and where $u_t = \pi_t^0(\theta_t)$, $c_t(\cdot)$ is the instantaneous cost function and $c_T(\cdot)$ is the terminal cost. We assume the incremental cost to be quadratic in control, such that $c_t(\theta_t, u_t) = l_t(\theta_t) + \frac{1}{2} u_t^T R u_t$.

Iterative Linear Quadratic Regulator (iLQR)

The iLQR Algorithm (Todorov and Li, 2005) iteratively solves a linear quadratic regulator problem which converges to the optimal solution of the original nonlinear optimization problem. A quick summary of the algorithm is given as follows:

1. Forward Pass: Given a nominal control sequence $\{u_t\}_{t=0}^{T-1}$ and initial state vector θ_0, the state is propagated using the dynamics $\theta_{t+1} = f(\theta_t, u_t, d_t)$ to obtain the nominal trajectory $(\bar{\theta}_t, \bar{u}_t)$.

2. Local LTV System Identification: The local LTV system around the nominal trajectory $(\bar{\theta}_t, \bar{u}_t)$ can be written as: $\delta\theta_{t+1} = A_t \delta\theta_t + B_t \delta u_t$, where $A_t = \frac{\partial f(\theta,u)}{\partial \theta}|_{(\bar{\theta}_t, \bar{u}_t)} \in \mathbb{R}^{n_\theta \times n_\theta}$ and $B_t = \frac{\partial f(\theta,u)}{\partial u}|_{(\bar{\theta}_t, \bar{u}_t)} \in \mathbb{R}^{n_\theta \times n_u}$.

3. Backward pass: Now, the iLQR algorithm computes a local linear feedback optimal control for the identified LTV system by solving the discrete-time Riccati Equation. Given the terminal conditions and the local LTV model parameters (A_t, B_t), we can do a backward-in-time sweep to compute the corresponding optimal control for that trajectory as:

$$\delta u_t = -k_t - K_t \delta\theta_t, \tag{10}$$

$$k_t = (R_t + B_t^T V_{t+1} B_t)^{-1} (R_t \bar{u}_t + B_t^T v_{t+1}), \tag{11}$$

$$K_t = (R_t + B_t^T V_{t+1} B_t)^{-1} B_t^T V_{t+1} A_t, \tag{12}$$

where $R_t := \nabla_{uu}^2 c_t|_{(\theta_t, u_t)}$ and v_t and V_t are calculated as:

$$v_t = l_t + A_t^T v_{t+1} - A_t^T V_{t+1} B_t (R_t + B_t^T V_{t+1} B_t)^{-1} (B_t^T v_{t+1} + R_t \bar{u}_t), \tag{13}$$

$$V_t = Q_t + A_t^T (V_{t+1}^{-1} + B_t R_t^{-1} B_t^T)^{-1} A_t, \tag{14}$$

with the terminal conditions $v_T(\theta_T) = \frac{\partial c_T}{\partial \theta}|_{\theta_T}$, $V_T(\theta_T) = \nabla_{\theta\theta}^2 c_T|_{\theta_T}$ and $Q_t := \nabla_{\theta\theta}^2 c_t|_{(\theta_t, u_t)}$ and $l_t := \frac{\partial c_t}{\partial \theta}|_{(\theta_t, u_t)}$.

https://doi.org/10.26868/25222708.2023.1421

4. Update trajectory: We can now update the nominal control sequence using the control generated from the backward pass to obtain:

$$\bar{u}_t^{k+1} = \bar{u}_t^k + k_t + K_t(\theta_t^{k+1} - \theta_t^k), \tag{15}$$

$$x_0^{k+1} = \theta_0^k. \tag{16}$$

Finally, the total cost is computed to check the convergence criteria, and if the convergence criteria is not met, we reiterate the process by repeating the four steps.

Simulation Results

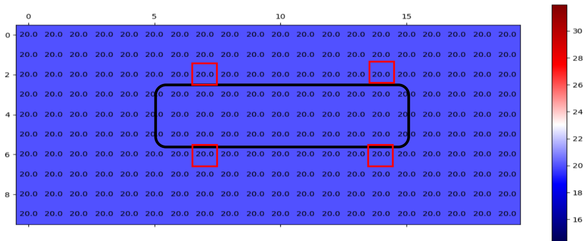

(a) Initial State

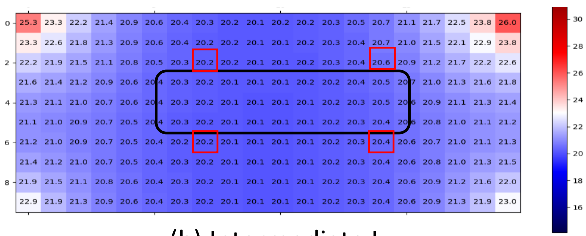

(b) Intermediate I

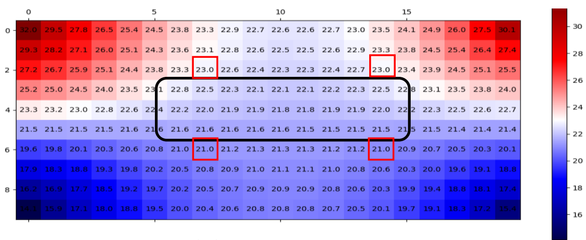

(c) Final State

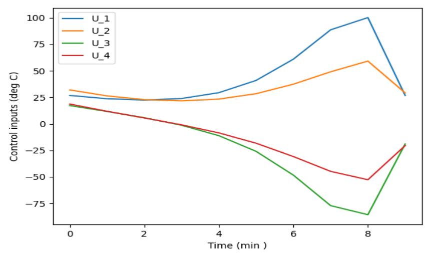

(d) Optimal Control Inputs

Figure 2: Linear Case 1: Room temperature heat maps derived from the PDE model, calibrated with experimental data and controlled using four heaters at the corners. The objective is to achieve the desired temperature values at four red boxes around the table.

In a case study, we verified the control strategy through simulations and evaluated its performance for various scenarios. We modeled the room as a 10 ft by 20 ft rectangle,

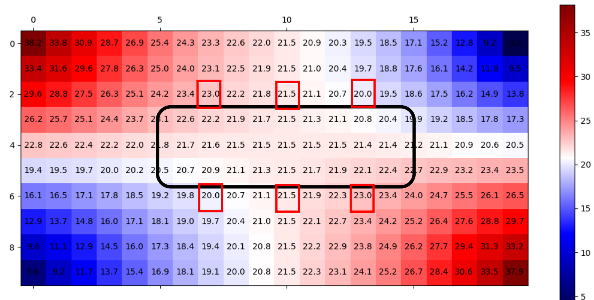

(a) Final State for linear case 2

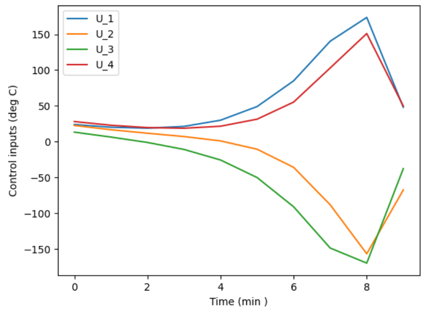

(b) Optimal Control Profile

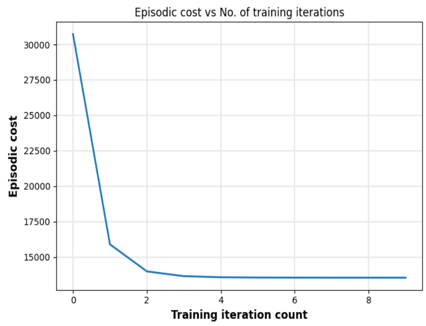

(c) Open-loop Convergence

Figure 3: Linear Case 2: Room temperature heat maps generated from the PDE model, calibrated with experimental data and controlled using four heaters at the corners. The objective is to attain the desired temperature values at six points around the table.

divided into uniform grids of 1 square foot size, with varying configurations of furniture and people placed in the room. A random selection of seats was occupied around the table. We assume that the room had actuators at each corner, i.e., heaters (heat sources) and coolers (heat sinks) that are used to create a temperature gradient profile. It is true that there is constant heat exchange in a room without any partition but a desired mean temperature profile with a small variation can still be maintained using external heat sources in different regions of the room. For example, imagine a room that has the sun on one side and thus the temperature near the wall facing the sun is always higher than the other walls of the room. For all the following cases, we set the initial room temperature to a uniform 20^oC.

Assuming no heat transfer across the walls, we rendered

https://doi.org/10.26868/25222708.2023.1421

the system thermally insulated during the actuator action. We performed simulations to evaluate the control performance for the selected occupancy and furniture configurations, and we analyzed the results to determine the effectiveness of the proposed control strategy.

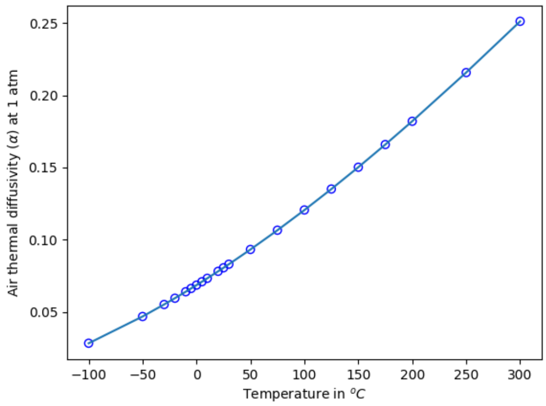

Figure 4: A cubic spline fit models the variation of the rmal diffusivity α as a function of temperature at 1 atm, b ased on the provided data.

Linear Heat Equation

The heat transfer is modeled using the dynamics described in Eq. 2. We simulated two cases for this system:

Case 1: Four seats around the table are assumed to be occupied, with desired temperatures set at 21°C, 21°C, 23°C, and 23°C. The actuators are activated and tasked with converging to the desired heat zones within 10 minutes of operation. Fig. 2 illustrates the evolution of the temperature profile towards the desired value, the optimal actuation scheme for each actuator, and the open-loop convergence for the ILQR algorithm.

Case 2: The number of occupants around the table is increased to six. In this case, the desired temperatures are set at 23°C, 21.5°C, 20°C, 20°C, 21.5°C, and 23°C respectively. Fig. 3 presents the final heatmap profile achieved, along with the optimal actuation scheme for each actuator.

Nonlinear Heat Equation

Although a linear model may be sufficient for simple experiments, in practice, the air inside a room with varying temperature profiles is not a homogeneous system. The diffusivity coefficient tends to change with temperature, leading to a nonlinear form of the heat diffusion PDE, as given in Eq. 1.
The temperature variation of the thermal diffusivity $\alpha(\theta)$ was found by fitting a cubic spline through the typical values of diffusivity of air at 1 atmospheric pressure, as shown in Fig. 4.

With the nonlinear heat transfer dynamics, we model the same room and set an initial ambient temperature of 20°C. The following cases are simulated:

Case 1: Five observers are seated around the table, and one observer is assumed to be standing next to a screen. The desired temperatures are set as 19°C, 19°C, 20°C, 20.5°C, 21°C, and 24°C, representing typical temperature setpoints during occupied load times.

Case 2: Maintaining the same initial condition, we modify the seating arrangement to have four users seated around the table. The desired temperatures are set as 21°C, 22°C, 23.5°C, and 24°C respectively.

The optimal actuation and final heatmap for the nonlinear cases are illustrated in Fig. 5.

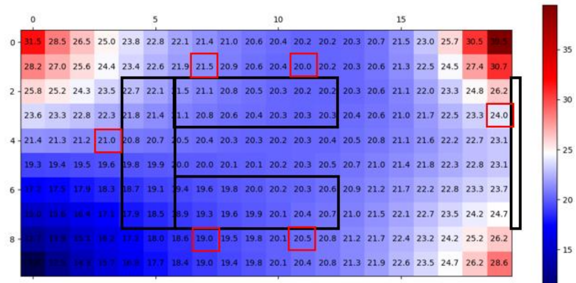

(a) Final State for nonlinear case 1

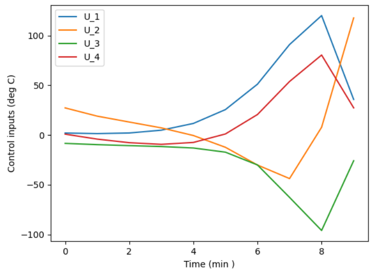

(b) Optimal Control Profile

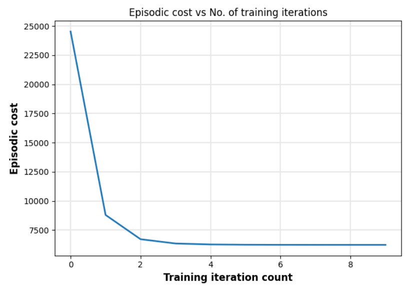

(c) Open loop Convergence

Figure 5: The desired temperature profiles for the nonli near case 1 configuration are set as the goal point. The o ptimal con-trol scheme and the final heatmap converge t o the desired set-points.

Disturbance Rejection

Once the desired heat profile is attained, the goal is to maintain the set temperatures while accounting for any external disturbances. Disturbances in building temperature can arise from various sources, such as occupants, other heat sources, or the HVAC system. Assuming these disturbances are minor, the resulting temperature variations can be treated as small perturbations around the equilibrium. By utilizing the feedback gains at the terminal state from the ILQR optimization, an LQR-based feedback control

https://doi.org/10.26868/25222708.2023.1421

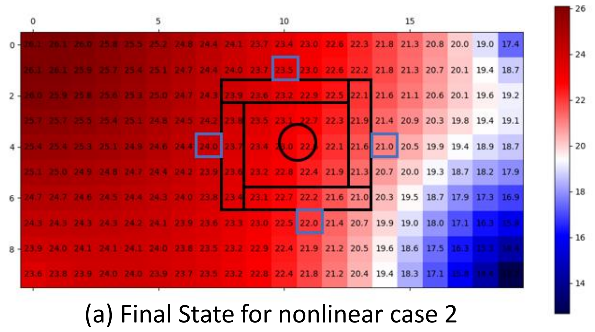

(a) Final State for nonlinear case 2

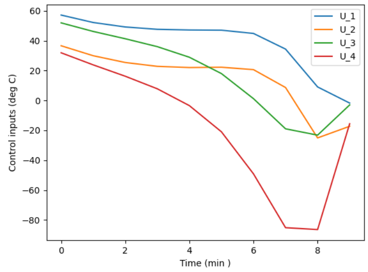

(b) Optimal Control Profile

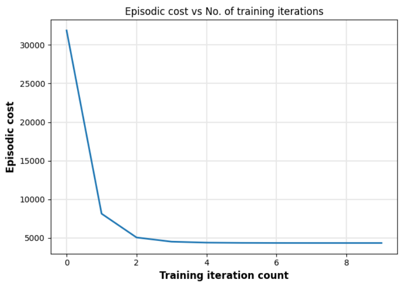

(c) Open loop Convergence

Figure 6: The desired temperature profiles for the nonli near case 2 configuration are set as the goal point. The o ptimal con-trol scheme and the final heatmap converge t o the desired set-points.

can be implemented to ensure disturbance rejection. As LQR is a well-established formulation, its details have been omitted due to space constraints.

Given the desired state x_T, and LQR feedback gain K, the optimal feedback controller for any time $t > T$ can be expressed as:

$$u_t = -K_T(x_t - x_T). \tag{17}$$

The effectiveness of disturbance rejection using this feedback law is illustrated in Fig. 7. In this scenario, we introduce a small disturbance after the terminal step of the ILQR control scheme. An LQR controller is formulated, and the feedback gain is applied. We observe that the controller is successful in rejecting the disturbance, and the system recovers the setpoints within the desired bounds.

Model Recalibration and Warm Starting

Since this PDE calibration technique relies on sensors to collect data, there is always a possibility of erroneous measurements leading to the misidentification of model parameters (in this case, α).

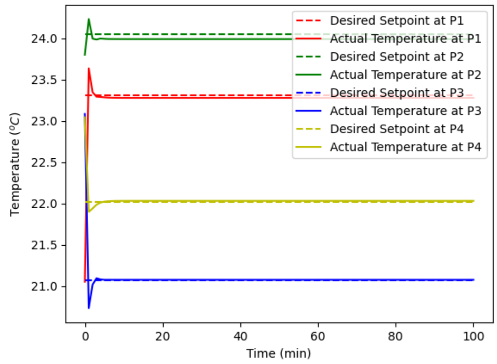

Figure 7: For nonlinear case 2, we introduce a small disturbance after the terminal step of the ILQR control scheme. An LQR controller is formulated and feedback gain is applied. It is observed that it is successful in rejecting the disturbance, and we recover the setpoints within the desired bounds.

Given an inaccurate model, the 'optimal' control actuation provided by the ILQR on that model is likely to fail to reach the target profiles when applied to the actual model, as illustrated in Fig 8 (b). In this scenario, the diffusion parameter α_1 is miscalibrated (with the true parameter being α_2). For such cases, misidentification still provides an opportunity for faster convergence of the ILQR algorithm. We can use the optimal trajectory obtained from the misidentified model as an *a priori* initial guess for the ILQR algorithm. By performing model recalibration and rerunning the control algorithm, ILQR can converge to the true optimal solution relatively quickly, as demonstrated in Fig 9.

Conclusion

In this paper, we presented a data-driven approach for optimally controlling sub-zonal, spatiotemporal temperature profiles in spacious rooms. Our methodology began with the calibration of a 2D diffusion Partial Differential Equation (PDE) model for heat transfer, utilizing Bluetooth Low Energy (BLE) sensor data (temperature and humidity) gathered from an experimental testbed. This calibrated model served as the basis for an iterative Linear Quadratic Regulator (iLQR) algorithm, which generated optimal control policies for each receding horizon in a model predictive control framework.

We demonstrated the effectiveness of our nonlinear control approach in maintaining desired spatiotemporal temperature profiles while mitigating the effects of external disturbances and noise. Our simulation results showcased the feasibility of optimally controlling heating systems, in linear and nonlinear cases, as well as its ability to reject disturbances, to achieve desired temperature distributions across various regions of a room. This data-driven method contributes to the development of more efficient and responsive building control systems that cater to occupant preferences and comfort.

Future research directions can include extending the ap-

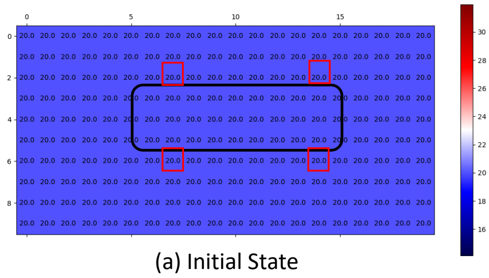

(a) Initial State

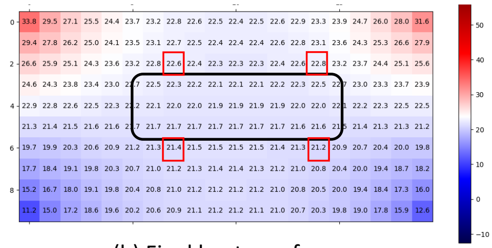

(b) Final heatmap for α_1

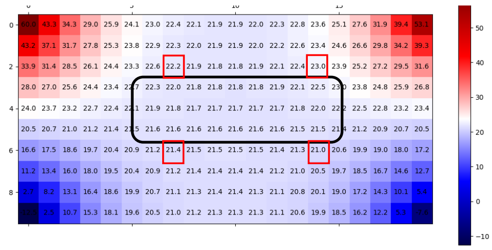

(c) Final heatmap for α_2

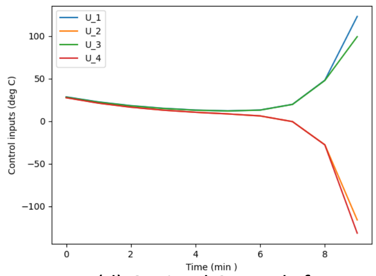

(d) Optimal Controls for α_1

Figure 8: Parametric uncertainty: Given the initial state (a), the PDE was mis-calibrated with the diffusion parameter α_1, resulting in the corresponding optimal controls and trajectory depicted in (b)-(c). When the obtained control inputs, shown in (d), for the mischaracterized model are applied to the true model, which has parameter α_2, the system diverges from the goal state.

proach to integrate with existing control systems, exploring different types of building systems, and investigating the impact of the proposed approach in non-building domains. Overall, the proposed data-driven approach offers a promising solution for addressing control problems in thermal management applications within large spaces with varying occupancy and preferences.

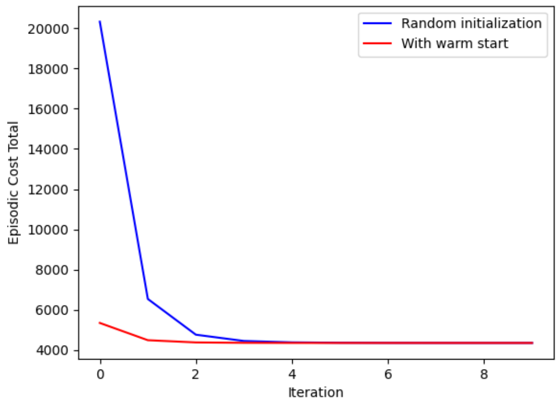

Figure 9: The optimal trajectory trained on the misidentified parameter system (α_1), when used to warm-start on the re-calibrated system (α_2) converges to the true optimal much faster than initializing from a random guess. Thus, the technique can handle model re-calibration relatively quickly.

References

Alla, A. and M. Falcone (2013). An adaptive pod approximation method for the control of advection-diffusion equations. In *Control and Optimization with PDE Constraints*, pp. 1–17. Springer.

Alla, A. and S. Volkwein (2015). Asymptotic stability of pod based model predictive control for a semilinear parabolic pde. *Advances in Computational Mathematics 41*(5), 1073–1102.

Banholzer, S., G. Fabrini, L. Grüne, and S. Volkwein (2020). Multiobjective model predictive control of a parabolic advection-diffusion-reaction equation. *Mathematics 8*(5), 777.

Baumann, M., P. Benner, and J. Heiland (2018). Space-time galerkin pod with application in optimal control of semilinear partial differential equations. *SIAM Journal on Scientific Computing 40*(3), A1611–A1641.

Casas, E. and K. Kunisch (2022). Infinite horizon optimal control problems for a class of semilinear parabolic equations. *SIAM Journal on Control and Optimization 60*(4), 2070–2094.

Casas, E., K. Kunisch, and F. Tröltzsch (2022). Optimal control of pdes and fe-approximation. *Numerical Control: Part A 23*, 115.

Griesse, R. and S. Volkwein (2005). A semi-smooth newton method for optimal boundary control of a nonlinear reaction-diffusion system msc–267.

He, R. and H. Gonzalez (2016). Gradient-based estimation of air flow and geometry configurations in a building using fluid dynamic adjoint equations. *arXiv preprint arXiv:1605.05339*.

Henderson, P., R. Islam, P. Bachman, J. Pineau, D. Precup, and D. Meger (2018). Deep reinforcement learning that matters. In *Thirty-Second AAAI Conference on Artificial Intelligence*.

Krstic, M. and A. Smyshlyaev (2008). Backstepping boundary control for first-order hyperbolic pdes and ap-

https://doi.org/10.26868/25222708.2023.1421

plication to systems with actuator and sensor delays. *Systems & Control Letters 57*(9), 750–758.

Kumar, P. R. and P. Varaiya (2015). *Stochastic systems: Estimation, identification, and adaptive control*, Volume 75. SIAM.

Leibfritz, F. and S. Volkwein (2007). Numerical feedback controller design for pde systems using model reduction: techniques and case studies. In *Real-time PDE-constrained optimization*, pp. 53–72. SIAM.

Qiao, H., X. Han, S. Nabi, and C. R. Laughman (2019). Coupled simulation of a room air-conditioner with cfd models for indoor environment. In *Proceedings of the 13th International Modelica Conference, Regensburg, Germany, March 4–6, 2019*, Number 157. Linköping University Electronic Press.

Renka, R. J., R. Renka, and A. Cline (1984). A triangle-based c^1 interpolation method. *The Rocky Mountain journal of mathematics*, 223–237.

Runxin, H. and G. Humberto (2016). Zoned hvac control via pde-constrained optimization [c]. In *ACC*, Number 7, pp. 587–592.

Sinha, S., R. Arora, and S. Roy (2000). Numerical simulation of two-dimensional room air flow with and without buoyancy. *Energy and Buildings 32*(1), 121–129.

Smyshlyaev, A. and M. Krstic (2010). *Adaptive control of parabolic PDEs*. Princeton University Press.

Stoll, M. and T. Breiten (2015). A low-rank in time approach to pde-constrained optimization. *SIAM Journal on Scientific Computing 37*(1), B1–B29.

Thong, P. C. S. (2023). Development of airflow simulation model and smart variable flow control schemes via adaptive vent/duct openings for efficient cooling and energy savings.

Tian, W., X. Han, W. Zuo, and M. D. Sohn (2018). Building energy simulation coupled with cfd for indoor environment: A critical review and recent applications. *Energy and Buildings 165*, 184–199.

Todorov, E. and W. Li (2005). A generalized iterative LQG method for locally-optimal feedback control of constrained nonlinear stochastic systems. In *Proceedings of American Control Conference*, pp. 300 – 306.

Van Schijndel, A. (2011). Multiphysics modeling of building physical constructions. In *Building Simulation*, Volume 4, pp. 49–60. Springer.

Volkwein, S. (2001). Optimal control of a phase-field model using proper orthogonal decomposition. *ZAMM-Journal of Applied Mathematics and Mechanics/Zeitschrift für Angewandte Mathematik und Mechanik: Applied Mathematics and Mechanics 81*(2), 83–97.

Wetter, M., M. Bonvini, T. S. Nouidui, and W. Zuo (2015). Modelica buildings library 2.0. In *Proc. of The 14th International Conference of the International Building Performance Simulation Association (Building Simulation 2015), Hyderabad, India*.

Zhai, Z., Q. Chen, P. Haves, and J. H. Klems (2002). On approaches to couple energy simulation and computational fluid dynamics programs. *Building and Environment 37*(8-9), 857–864.

Zuo, W., M. Wetter, W. Tian, D. Li, M. Jin, and Q. Chen (2016). Coupling indoor airflow, hvac, control and building envelope heat transfer in the modelica buildings library. *Journal of Building Performance Simulation 9*(4), 366–381.

https://doi.org/10.26868/25222708.2023.1421